

# Influence of composition and molecular structure on the microhardness of liquid crystalline copolymers

F. J. Baltá Calleja and C. Santa Cruz

*Instituto de Estructura de la Materia CSIC, Serrano 119, 28006 Madrid, Spain*

and D. Chen and H. G. Zachmann

*Institut für Technische und Makromolekulare Chemie, Universität Hamburg, Bundesstrasse 45, 2000 Hamburg 13, Germany*

*(Received 12 March 1990; revised 20 June 1990; accepted 6 September 1990)*

The mechanical properties of copolyesters of *p*-hydroxybenzoic acid (PHB) and poly(ethylene naphthalene-2,6-dicarboxylate) (PEN) and of PHB and poly(ethylene terephthalate) (PET) were investigated over a wide range of compositions using the microhardness technique. The mechanical behaviour has been interpreted in terms of an aggregate model of additive units of structure. On this basis the changes in microhardness with composition can be related to the following factors: degree of crystallinity, crystal thickness and polymorphic crystal forms. In the case of the amorphous materials the increase of the microhardness with increasing number of flexible chain sequences (PET, PEN) has been discussed in terms of a simple additive behaviour of single components PET/PHB and PEN/PHB. In the case of the crystallized materials it is shown that the hardness of the PET and PEN crystals is an increasing function of the crystallite dimensions (flexible chain domains).

**(Keywords: molecular structure; liquid crystals; microhardness)**

## INTRODUCTION

Liquid crystalline polymers (LCPs) are of growing interest in polymer science<sup>1-3</sup>. This attention is due to both the scientific and practical importance of LCPs. From the viewpoint of practical applications, LCPs are very attractive as potential high performance materials for use in high modulus engineering plastics and fibres<sup>1</sup>, or for the production of displays and other optoelectronic devices<sup>4</sup>. In recent years interest in rigid chain thermotropic liquid crystalline copolymers has grown considerably<sup>5,6</sup>. Of particular interest has been the copolyester prepared from hydroxybenzoic acid and 2-hydroxy-6-naphthoic acid which form thermotropic liquid crystalline melts which can readily be processed into highly oriented fibres or films<sup>7</sup>. Dielectric properties, dynamic mechanical behaviour, experimental and theoretical longitudinal chain moduli and thermal measurements of these random copolymers have been reported<sup>8-11</sup>.

Copolyesters of poly(ethylene naphthalene-2,6-dicarboxylate) (PEN) and *p*-hydroxybenzoic acid (PHB), containing different amounts of PHB, have been studied<sup>12</sup> using real time X-ray diffraction and calorimetric techniques. In addition, copolyesters of poly(ethylene terephthalate) (PET) with different amounts of PHB were studied by n.m.r. and neutron scattering experiments<sup>12</sup>. In the materials containing up to 50% PHB, crystals of PET and/or PEN are formed<sup>12</sup>. In those containing 80-90% PHB, only crystals of PHB are detected. It is now of interest to study the influence of

the glassy liquid crystalline structure on the microhardness of these materials. Microhardness is a technique which can offer direct information on microstructural changes in semicrystalline and amorphous polymers<sup>13-15</sup>. In addition, hardness of polymers can be correlated with many of their mechanical properties<sup>13-16</sup>, which makes such measurements a fast and convenient method for material characterization. Microhardness has also been proved to detect polymorphic phase changes in polymers<sup>17</sup>, and especially changes in polymer blends with composition<sup>18,19</sup>. In this paper we report the results of a study of the influence of the composition and the molecular structure on the microhardness of the above series of copolyesters (PET/PHB, PEN/PHB).

## EXPERIMENTAL

### *Preparation of specimens*

Samples of random PET/PHB and PEN/PHB were synthesized as described elsewhere<sup>12</sup>. Amorphous films were obtained by melt pressing 10°C above the melting point and quenching in ice water. Crystallized samples were prepared by annealing the amorphous samples for 4 h, 20°C below the melting point of each respective copolymer. While PET forms only one crystalline modification, the crystals of PEN show two modifications: the  $\alpha$  modification with density  $\rho_\alpha = 1.40 \text{ g cm}^{-3}$  containing one molecule per unit cell and the  $\beta$  modification with  $\rho_\beta = 1.435 \text{ g cm}^{-3}$  and four molecules per unit cell.

## Specimen characterization

Density was measured with a gradient column at room temperature using a mixture of n-hexane and carbon tetrachloride. The degree of crystallinity,  $\alpha$ , was calculated from the amorphous density measured on quenched samples (see Tables 1 and 2) and from the crystalline density derived from the crystal lattice cell.

The X-ray diffraction patterns of the amorphous materials show the existence of one characteristic broad scattering maximum. Ehrenfest's relation was applied for the derivation of the spacing  $d$ , denoting the frequently occurring interatomic distance in a largely disordered polymer. In addition, the coherence length,  $D$ , was obtained from X-ray line broadening data using Scherrer's formula  $D = \lambda/\beta_0 \cos \theta$ , where  $\lambda$  is the wavelength of the radiation used,  $\beta_0$  the integral breadth of the scattering halo in radians and  $\theta$  is the Bragg angle.

For the study of small angle X-ray scattering (SAXS) from the crystallized materials a Kratky compact camera and a detector with energy discrimination were used. Scattering of nickel filtered Cu-K $\alpha$  radiation was measured using two different entrance slit heights of 60 and 130  $\mu\text{m}$  in overlapping angular regions of  $0.013 \text{ nm}^{-1} < s < 0.1 \text{ nm}^{-1}$  and  $s > 0.08 \text{ nm}^{-1}$  respectively ( $s = 2 \sin \theta/\lambda$ ). The width of the counter slit was taken to be 2.5 times the value of the entrance slit height in each angular region. Finally, both scattering regions were normalized to each other in absolute units.

Figure 1 shows the resulting small angle scattering curves for the samples of PEN/PHB and PET/PHB. For the determination of the long period,  $L$ , the correlation

function was calculated using the Strobl method<sup>20</sup>. The value of  $L/2$  is given by the position of the first minimum in the correlation curve. From the depth of the correlation function at its first minimum, as it is generally known, the product  $\alpha_L(1 - \alpha_L)$  can be determined.  $\alpha_L$  represents the linear crystallinity, i.e. the degree of crystallinity within the stacked lamellae. This value is usually larger than the degree of crystallinity  $\alpha$  as determined from density or wide angle X-ray scattering (WAXS), because in addition to the amorphous regions between the crystal lamellae, larger amorphous regions outside the stacked

**Table 1** Experimental values for the densities of quenched ( $\rho_{\text{que}}$ ) and crystallized ( $\rho_{\text{cryst}}$ ) materials, the temperature at which the samples were crystallized for 4 h ( $T_c$ ) and the degree of crystallinity ( $\alpha$ ) derived from density for PET/PHB samples, as a function of molar composition

PET/PHB	$\rho_{\text{que}}$ (g cm $^{-3}$ )	$T_c$ (°C)	$\rho_{\text{cryst}}$ (g cm $^{-3}$ )	$\alpha$
100/0	1.3376	240	1.4081	0.49
90/10	1.3402	220	1.3924	0.37
80/20	1.3432	210	1.3908	0.35
70/30	1.3407	200	1.3821	0.30
60/40	1.3688	215	1.3929	0.22
50/50	1.3760	210	1.3978	0.20
40/60	1.3905	180	1.4010	0.11
30/70	1.3984	200	1.4007	—

**Table 2** Experimental values for the densities of quenched ( $\rho_{\text{que}}$ ) and crystallized ( $\rho_{\text{cryst}}$ ) materials, the temperature at which the samples were crystallized for 4 h ( $T_c$ ) and the degree of crystallinity ( $\alpha$ ) derived from density for PEN/PHB samples, as a function of molar composition

PEN/PHB	$\rho_{\text{que}}$ (g cm $^{-3}$ )	$T_c$ (°C)	$\rho_{\text{cryst}}$ (g cm $^{-3}$ )	Crystal form	$\alpha$
100/0	1.3281	220	1.3565	$\alpha$	0.38
100/0	1.3281	250	1.3653	$\beta$	0.37
90/10	1.3314	210	1.3885	$\alpha$	0.37
90/10	1.3314	240	1.3610	$\beta$	0.30
80/20	1.3324	220	1.3584	$\alpha$	0.36
80/20	1.3324	180	1.3644	$\beta$	0.33
70/30	1.3598	200	1.3742	$\alpha$	0.31
70/30	1.3598	230	1.3817	$\beta$	0.30
60/40	1.3688	190	1.3748	$\alpha$	0.16
60/40	1.3688	220	1.3802	$\beta$	0.18
50/50	1.3714	220	1.3777	$\alpha$	0.18

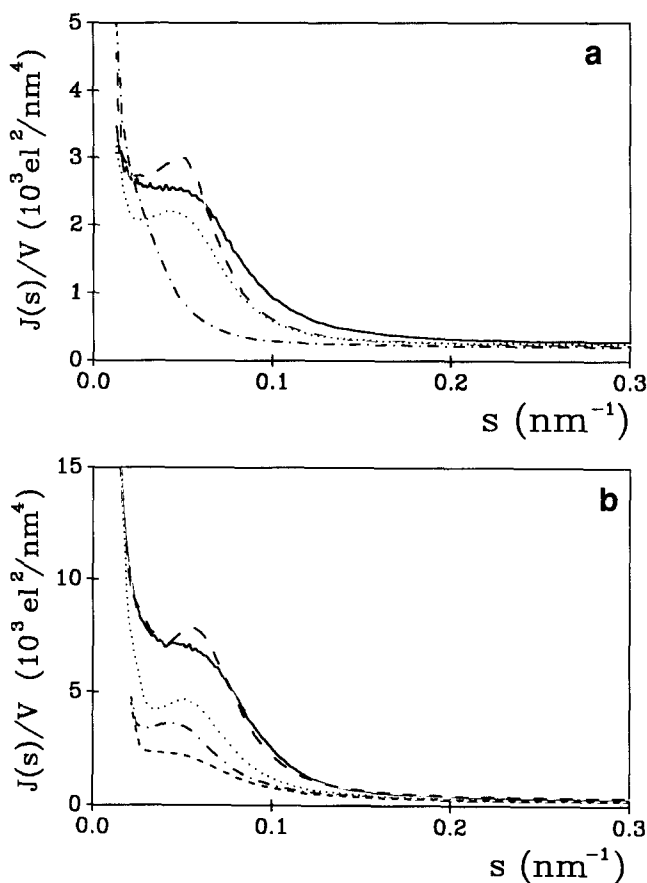


**Figure 1** Angular dependence of absolute small angle scattering for (a) PEN/PHB and (b) PET/PHB copolymers. —, Pure homopolymers (PEN, PET); —, 90/10 copolymers; ····, 80/20 copolymers; - - - -, 60/40 copolymers; - - - -, 50/50 copolymers

lamellae may be present<sup>21</sup>. From the SAXS data alone, it is not possible to determine which of the two values,  $\alpha_L$  or  $1 - \alpha_L$ , is the crystalline fraction and which is the amorphous fraction. The choice is usually made by comparing the above data with the value of  $\alpha$  as determined from density<sup>22</sup>. In this work the  $\alpha_L$  value was chosen in such a way that it would be consistent with the crystallinity value derived from density (Tables 1 and 2). In addition to the comparison to density we have also compared the crystal thickness,  $l_c$ , results with the average sequence lengths of PET and PEN units respectively. Finally,  $l_c$  was derived from  $l_c = \alpha_L L$ .

#### Microhardness measurements

Microhardness was measured at room temperature using a Vickers tester. The test uses a squared pyramidal diamond with included angles  $\tau$  between non-adjacent faces of the pyramid of 136°. The microhardness is given by:

$$H = 2 \sin(\tau/2)P/d^2 = 1.854P/d^2 \quad (1)$$

where  $P$  is the force in Newtons and  $d$  is the diagonal length of the impression in metres. The force is applied at a controlled rate, held for 0.1 min, and removed. The length of the impression is measured to  $\pm 1 \mu\text{m}$  with a microscope equipped with a filar eyepiece. Loads of 0.15, 0.25, 0.5 and 1 N were used.

## RESULTS

The PEN/PHB copolyesters containing <60 mol% PHB are completely amorphous when quenched from the melt in ice water. When annealed at appropriate temperatures the PEN sequences crystallize while all PHB sequences remain in the amorphous regions<sup>12</sup>. Similar results are obtained for the PET/PHB copolyesters. Here, only PET is capable of crystallizing.

On the other hand, the copolyesters containing >60 mol% PHB, even when they are quenched from 320°C, contain small, strongly distorted PHB crystals which lead to a small reflection superposed on the amorphous halo. Therefore, these samples cannot be considered to be amorphous even after quenching. No change in crystallinity is observed upon annealing. The PEN and the PET units remain in the amorphous regions.

Tables 1 and 2 show the experimental values for the densities of quenched and crystallized materials, the temperature of crystallization and the degree of crystallinity of the PET/PHB and PEN/PHB copolymers respectively containing <40 mol% PHB. The structural data derived from the WAXS maxima of the two series of quenched copolymers are given in Tables 3 and 4. The long period, crystal thickness and linear crystallinity derived from SAXS results (see Figure 1) for the crystallized samples are shown in Tables 5 and 6. In addition, the average length values,  $l_c^* = nc$  (where  $n$  = average number of repeating units and  $c$  = unit cell dimension along the chain axis) of PET and PEN sequences, as derived from simple statistical calculations, are listed. It is seen that the values of  $l_c$  for both series of copolymers are related to the average value,  $l_c^*$ , of PET and/or PEN sequences which are capable of crystallizing.

Figure 2 shows the variation of  $H$  (microhardness of the crystallized samples) and  $H_a$  (microhardness of quenched amorphous samples) as a function of PET

**Table 3** Experimental values of the scattering angle ( $\theta$ ), interatomic distance ( $d_i$ ), integral breadth ( $\beta_0$ ) and cluster size ( $D$ ) for PET/PHB amorphous copolymers

PET/PHB	$\theta$ (°)	$d_i$ (Å)	$\beta_0$ (rad)	$D$ (Å)
100/0	10.3	5.4	0.123	12.7
90/10	10.3	5.4	0.113	13.9
80/20	10.2	5.4	0.109	14.4
70/30	10.2	5.4	0.083	15.6
60/40	10.2	5.4	0.086	18.2
50/50	10.1	5.5	0.068	23.0
40/60	10.0	5.5	0.050	31.3

**Table 4** Experimental values of scattering angle ( $\theta$ ), interatomic distance ( $d_i$ ), integral breadth ( $\beta_0$ ) and cluster size ( $D$ ) for PEN/PHB amorphous copolymers

PEN/PHB	$\theta$ (°)	$d_i$ (Å)	$\beta_0$ (rad)	$D$ (Å)
100/0	10.7	5.2	0.115	13.6
90/10	10.5	5.4	0.108	14.5
80/20	10.5	5.4	0.105	15.0
70/30	10.2	5.5	0.096	16.3
60/40	10.0	5.5	0.087	18.0
50/50	10.0	5.5	0.078	20.0

**Table 5** Experimental values of long period ( $L$ ), crystal thickness ( $l_c$ ), linear crystallinity ( $\alpha_L$ ) for copolymers PET/PHB and the calculated sequence length ( $l_c^*$ )

PET/PHB	$L$ (Å)	$l_c$ (Å)	$\alpha_L$	$l_c^*$ (Å)
100/0	90	57	0.64	$\infty$
90/10	112	41	0.37	$97 \pm 40$
80/20	120	36	0.30	$43 \pm 20$
60/40	112	29	0.26	$16 \pm 10$
50/50	113	25	0.22	$14 \pm 8$

**Table 6** Experimental values of long period ( $L$ ), crystal thickness ( $l_c$ ), linear crystallinity ( $\alpha_L$ ) for copolymers PEN/PHB and the calculated sequence length ( $l_c^*$ )

PEN/PHB	$L$ (Å)	$l_c$ (Å)	$\alpha_L$	$l_c^*$ (Å)
100/0	112	77	0.69	$\infty$
90/10	144	67	0.47	$124 \pm 55$
80/20	125	52	0.42	$55 \pm 27$
60/40	110	43	0.39	$21 \pm 13$

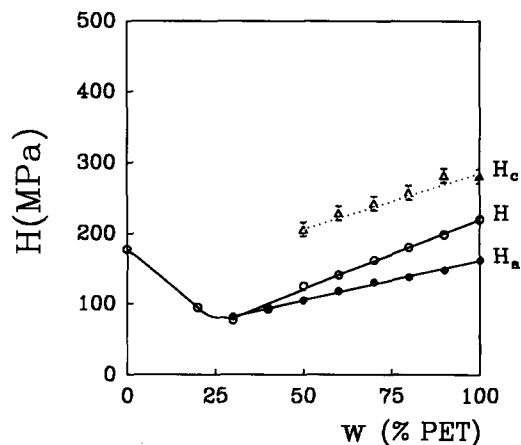


**Figure 2** Change of microhardness of PET/PHB copolymers as a function of PET concentration. ●, amorphous material ( $H_a$ ); ○, crystallized material ( $H$ ); △, PET crystals

content ( $w_{\text{PET}}$ ). For PET concentrations  $w_{\text{PET}} > 30\%$ , where the samples are amorphous,  $H_a$  linearly increases with the increasing concentration of PET units according to:

$$H_a = H_0 + kw_{\text{PET}} \quad (2)$$

where the intercept  $H_0 \approx 50$  MPa and  $k = H_a - H_0$  is the slope of the plot. On the other hand, for  $w_{\text{PET}} < 30\%$ , where the amorphous matrix contains small PHB crystals, the microhardness increases with increasing number of PHB sequences up to  $H = 178$  MPa for 100% PHB ( $\alpha_{\text{PHB}} = 85\%$ ). Furthermore, the microhardness of the crystallized samples,  $H$ , also shows a linear increase with  $w_{\text{PET}}$  within the  $w_{\text{PET}} > 30\%$  range:

$$H = H'_0 + qw_{\text{PET}} \quad (3)$$

with a slope  $q > k$ . In addition, the microhardness of the crystals,  $H_c$ , was calculated using the additivity relation for each composition  $w_{\text{PET}}$ :

$$H = H_c\alpha + H_a(1 - \alpha) \quad (4)$$

It is seen that  $H_c$  for the PET crystals gradually decreases with increasing PHB concentration down to  $w_{\text{PET}} \approx 50\%$ , the composition at which the smallest crystals are obtained<sup>12</sup>. From Table 5 it is clearly seen that the decrease in  $H_c$  can be correlated with the decrease in crystal thickness of the PET domains.

The situation with the PEN/PHB copolymers is somewhat more complex because the PEN crystals may appear either as fully crystallized in the  $\alpha$  modification or almost totally crystallized in the  $\beta$  modification. Both modifications show a triclinic symmetry<sup>6</sup>. Figure 3 illustrates the variation of  $H$  and of  $H_a$  as a function of PEN content. The crystal microhardness values  $H_c^\alpha$ ,  $H_c^\beta$  were calculated assuming that equation (4) also holds for these systems. As in the case of PET/PHB copolymers, we obtain a linear increase of  $H_a$  with  $w_{\text{PEN}}$ . However, in this case for  $w_{\text{PEN}} > 50\%$ :

$$H_a = H_0 + rw_{\text{PEN}} \quad (5)$$

where  $H_0 \approx 10$  MPa and  $r = H_a - H_0$  is the slope of the plot. In addition, the microhardness values of the crystallized materials,  $H_\alpha$  and  $H_\beta$ , show a linear increase for  $w_{\text{PEN}} > 50\%$ . It is noteworthy that the microhardness data in Figure 3 show nearly the same minima for the

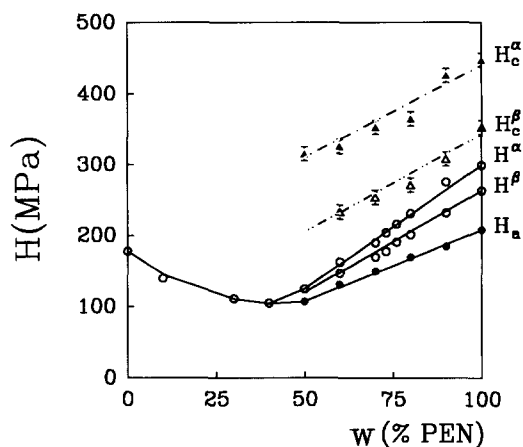


**Figure 3** Variation of microhardness of PEN/PHB copolymers as a function of PEN concentration. ●, Amorphous material ( $H_a$ ); ○, crystallized material with PEN  $\beta$  and  $\alpha$  crystals; △, crystal hardness for PEN  $\beta$  crystal; ▲, crystal hardness for PEN  $\alpha$  crystals

amorphous and crystallized samples at a concentration  $w_{\text{PEN}} \approx 50\%$ .

By using equation (4) for each pair of  $H$  and  $H_a$  values for each crystalline phase and every concentration, we finally obtain the values for the crystal microhardness of both phases depending on  $w_{\text{PEN}}$ . As in the case of PET/PHB, the  $H_c$  values for both modifications gradually decrease with increasing PHB concentration until the concentration  $w_{\text{PEN}} \approx 50\%$  is reached. Here the PEN crystals are not detected anymore<sup>12</sup>. The decrease in  $H_c$  for the PEN/PHB series can also be correlated to the crystal thickness decrease shown in Table 6.

## DISCUSSION

### Dependence of $H_a$ on composition

In the case of the amorphous samples the most frequently occurring interatomic distance  $d_i$ , remains practically constant with increasing  $w_{\text{PET}}$  (Table 3), i.e. the increasing concentration of rigid PHB units within the material does not substantially affect the overall average molecular packing, although the density increases. This change in density must be caused by a corresponding change in the free volume. On the other hand, since both  $\rho_{\text{que}}$  (quenched samples) and the coherence length,  $D$ , within the amorphous domains decrease with increasing concentration of PET units, the changes in  $\rho_{\text{que}}$  and  $D$  cannot be responsible for the increase of  $H_a$  with  $w_{\text{PET}}$  in Figure 2. This result is at variance with earlier data on semicrystalline polymers showing that a density rise always leads to a microhardness increase<sup>13,14</sup>. A similar structural trend for the amorphous samples of PEN/PHB is obtained (Figure 3). Thus, the interatomic distance  $d_i$  is nearly independent of  $w_{\text{PEN}}$  and the density and the cluster size,  $D$ , of the amorphous domains decrease with increasing number of PEN units.

As it is not possible to explain the variation of microhardness by differences in the densities, we have to look for another possible interpretation. It seems that the dependence of  $H_a$  on composition could, in principle, be explained in terms of a simple additive behaviour of the single components  $H_a^{\text{PET}}$ ,  $H_a^{\text{PHB}}$ . When we consider the dependence of  $H_a$  on the PET content in the PET/PHB quenched and amorphous (see Figure 2) we find a linear decrease of the microhardness with decreasing PET content down to 40% PET. By extrapolation this decrease yields a value of  $H_a^{\text{PHB}} = 50$  MPa for a fully amorphous PHB. The dependence of  $H_a$  on composition is well described by the relation:

$$H_a = H_a^{\text{PET}}w_{\text{PET}} + H_a^{\text{PHB}}w_{\text{PHB}} \quad (6)$$

Such an equation follows the predictions of a mechanical parallel model<sup>13</sup> and simply states the additivity of the values of the two independent microhardness components.

A similar relation is obtained for the PEN/PHB copolyesters (Figure 3). However, in this case, by extrapolation to  $w_{\text{PEN}} = 0$ , a value of  $\sim 10$  MPa is obtained for amorphous PHB. This value does not quite agree with the previous value obtained from the microhardness plot of PET/PHB. The difference seems to be larger than the experimental error of extrapolation. Therefore, we have to assume that the simple additivity of the microhardness values, as given by equation (6),

does not hold strictly. However, in spite of these deviations there exists good support for the conclusion that the microhardness of amorphous PHB is smaller than the values of PET and PEN and is probably in the region of 10–50 MPa. A direct measurement of the microhardness of amorphous PHB cannot be performed because it is not possible to obtain this material in the amorphous state. A value of  $H = 178$  MPa was measured for the highly crystalline (85%) PHB sample (see Figures 2 and 3). At this stage it is worth pointing out that a strictly linear dependence of microhardness on composition has been found for quenched PEN/PET copolyesters<sup>23</sup>.

Let us now turn to the increase of  $H$  with decreasing PET and/or PEN content seen in Figures 2 and 3 respectively. While in this region no crystals of PET or PEN are present there is an indication based on d.s.c. and X-ray scattering measurements that small PHB crystals in the hexagonal form exist which become better ordered and more abundant with increasing PHB content. Therefore, this part of the microhardness curves cannot be considered to represent the microhardness of truly amorphous copolyesters. As a consequence, we attribute this increase of microhardness with increasing PHB content to the presence of these PHB crystals.

#### Dependence of $H$ on composition

The larger values of  $H$  for the crystallized samples are correlated with the formation of PET and PEN crystals<sup>12</sup>. With increasing number of PET units the degree of crystallinity increases because the probability of longer PET sequences agglomerating to form crystalline regions also increases. The concurrent increase of both crystallinity ( $\alpha$ ) and crystal thickness ( $l_c$ ) (Tables 1, 5) with increasing PET units ( $w_{PET}$ ) yields increasingly large  $H$  values (Figure 2). As a result, the slope  $q$  in equation (3) is larger than  $k$  in equation (2). A similar tendency for the  $H$  values of PEN/PHB materials is detected (Figure 3). Here the larger values of  $H^\alpha$  and  $H^\beta$  for the crystallized samples are connected with the formation of PEN crystals in both polymorphic forms.

#### Dependence of $H_c$ on crystal thickness

The value of  $H_c$  has previously been derived for polyethylene<sup>14</sup> and polypropylene<sup>17</sup> by means of equation (4). In the case of the poly(ethylene terephthalate) homopolymer it has been shown that this equation can only be applied if  $\alpha$  is replaced by the linear crystallinity,  $\alpha_L$ , within the lamellae stacks<sup>21</sup>. However, for the present series of copolyesters values of  $\alpha$  and  $\alpha_L$  are not far from each other (see Tables 1, 2, 5 and 6) and equation (4) can be applied in either case. For the PET homopolymer  $\alpha_L$  is somewhat larger than  $\alpha$ . Nevertheless, the calculated  $H_c$  values, when using  $\alpha$  or  $\alpha_L$ , differ by no more than 5%. In the case of the PEN homopolymer a larger difference between  $\alpha_L$  and  $\alpha$  is found. For consistency, we have also taken the  $\alpha$  value to calculate  $H_c$ .

It is noteworthy that the  $H_c$  values calculated by means of equation (4) do increase with increasing PET content (see Figure 2). This is obviously a consequence of the increase of the crystal thickness,  $l_c$ , with increasing  $w_{PET}$  (see Table 5). According to previous investigations on PE<sup>14</sup> and PP<sup>19</sup>, the dependence of  $H_c$  on  $l_c$  can be

assumed to be given by:

$$H_c = H_c^\infty / (1 + b/l_c) \quad (7)$$

From a plot of  $1/H_c$  versus  $1/l_c$  (Figure 4) one obtains values of  $H_c^\infty = 380$  MPa which represents the microhardness of infinite PET crystals and  $b = 19$  Å which characterizes the depression from this value due to the finite crystal thickness. Equation (7) is justified on the basis of a heterogeneous deformation model involving the heat dissipated by the plastically deformed crystals<sup>14</sup>. The  $H_c^\infty$  and  $b$  values given above fit quite well with previous data obtained for pure PET materials crystallized from the glassy state<sup>21</sup>.

In the case of PEN/PHB copolyesters the values of  $H_c$  also depend on crystal thickness for both polymorphic forms. Figure 5 illustrates the plot of  $1/H_c$  versus  $1/l_c$  which yields a common value of  $H_c^\infty = 880$  MPa for both forms with parameters  $b_\alpha = 73$  Å and  $b_\beta = 117$  Å. It is noteworthy that  $H_c^\infty$  for PEN is the largest limiting microhardness found for any polymer so far, and in fact lies close to the value for hard metals (nickel, copper, mild steel).

Finally it is worth pointing out that when applying equation (4) one has to take into consideration that during crystallization the PHB units are rejected from

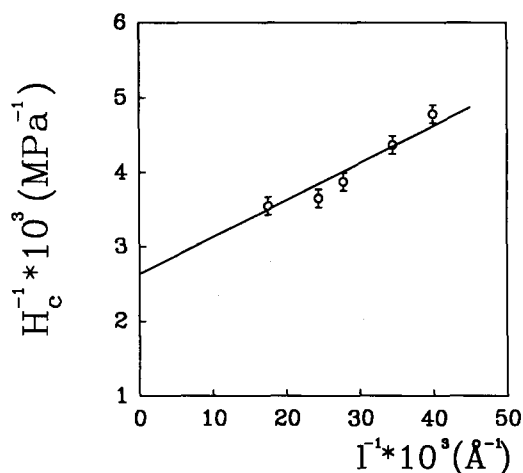


Figure 4 Variation of reciprocal crystal hardness for PET crystals as a function of reciprocal crystal thickness

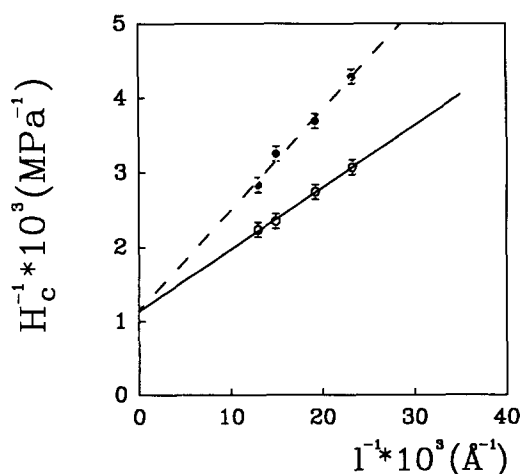


Figure 5 Variation of reciprocal crystal hardness for the PEN  $\alpha$  (○) and  $\beta$  crystals (●) as a function of reciprocal crystal thickness

the crystals. As a consequence the fraction of PHB units within the amorphous phase of the semicrystalline material is larger than in the completely amorphous material. Therefore, according to the dependence of  $H_a$  on the concentration of PHB shown in *Figure 2*, the value for each  $H_a$  data point to be inserted in equation (4) should be slightly smaller than that for the amorphous material before crystallization. If this is done one would obtain for PET the values of  $H_c^\infty = 350$  MPa and  $b = 6$  Å, and for the  $\alpha$  and the  $\beta$  forms of PEN the values  $H_c^\infty = 820$  MPa,  $b_\alpha = 60$  Å and  $H_c^\infty = 640$  MPa,  $b_\beta = 62$  Å respectively. Although the rejection of the PHB units from the crystals slightly affects the  $H_c^\infty$  and  $b$  values it does not influence the proposed interpretation in terms of equation (7).

## CONCLUSIONS

In summary, the hardness of PET/PHB and PEN/PHB quenched copolymers show microhardness minima for concentrations 30/70 to 50/50 respectively, due to the fact that the samples are fully amorphous for these compositions. If one increases the PET, or the PEN content the microhardness will increase owing either to the additive behaviour of the single components for amorphous samples, or to the increasing crystal thickness in the case of crystallized samples. If, on the other hand, one increases the PHB concentration the samples always crystallize and the crystallite-reinforced material shows a microhardness increase which is proportional to the PHB crystal content.

## ACKNOWLEDGEMENTS

The authors express their thanks to the Internationales Büro, Kernforschungsanlage, Karlsruhe and to CSIC, Madrid for the generous support of this Cooperation Project. Grateful acknowledgement is also due to

CICYT, Spain for the support of this investigation (grant no. MAT 88-0151).

## REFERENCES

- 1 Windle, A. *MRS Bull.* 1987, **12**, 18
- 2 Ciferri, A., Krigbaum, W. R. and Meyer, R. B. (Eds) 'Polymer Liquid Crystals', Academic Press, London, 1982, p. 1
- 3 Chapoy, L. L. 'Recent Advances in Liquid Crystalline Polymers', Elsevier, London, 1984
- 4 Coles, H. J. in 'Developments in Crystalline Polymers' (Ed. D. C. Bassett), Elsevier, London, 1988, p. 115
- 5 Dobb, M. G. and McIntyre, J. E. *Adv. Polym. Sci.* 1984, **60/61**, 61
- 6 Finkelmann, H. and Rehage, G. *Adv. Polym. Sci.* 1984, **60/61**, 99
- 7 Calundann, G. and Jaffe, M. in 'Proc. Conf. Chem. Res. XXVI, Synthetic Polymers', Houston, Texas, 1989, p. 30
- 8 Alhaj-Mohammed, M. H., Davies, G. R., Abdul Jawad, S. and Ward, I. M. *J. Polym. Sci., Polym. Phys. Edn* 1988, **26**, 1751
- 9 Troughton, M. J., Davies, G. R. and Ward, I. M. *Polymer* 1989, **30**, 58
- 10 Troughton, M. J., Unwin, A. P., Davies, G. R. and Ward, I. M. *Polymer* 1988, **29**, 1389
- 11 Davies, G. R. and Ward, I. M. in 'High Modulus Polymers: Approaches to Design and Development', Marcel Dekker, New York, 1988, p. 37
- 12 Buchner, S., Di, C., Gehrke, R. and Zachmann, H. G. *Mol. Cryst. Liq. Cryst.* 1988, **155**, 357
- 13 Baltá Calleja, F. J. *Adv. Polym. Sci.* 1985, **66**, 117
- 14 Baltá Calleja, F. J. and Kilian, H. G. *Colloid Polym. Sci.* 1985, **263**, 697
- 15 Baltá Calleja, F. J., Martínez Salazar, J. and Rueda, D. R. 'Encyclopaedia of Polymer Science and Engineering', 2nd Edn, John Wiley, 1987, p. 614
- 16 Baltá Calleja, F. J. and Kilian, H. G. *Colloid Polym. Sci.* 1988, **266**, 29
- 17 Baltá Calleja, F. J., Martínez Salazar, J. and Asano, T. *J. Mater. Sci. Lett.* 1988, **7**, 165
- 18 Martínez Salazar, J., Garcia Tijero, J. M. and Baltá Calleja, F. J. *J. Mater. Sci.* 1988, **23**, 862
- 19 Baltá Calleja, F. J., Santa Cruz, C., Sawatari, C. and Asano, T. *Macromolecules* 1990, **23**, 5352
- 20 Strobl, G. R. and Schneider, M. J. *J. Polym. Sci.* 1980, **18**, 1343
- 21 Santa Cruz, C., Baltá Calleja, F. J., Zachmann, H. G. and Asano, T. *J. Polym. Sci. Phys.* in press
- 22 Kortleve, G. and Vonk, C. G. *Kolloid Z. Z. Polym.* 1968, **225**, 124
- 23 Santa Cruz, C., Baltá Calleja, F. J., Zachmann, H. G. and Chen, D. *J. Mater. Sci.* in press